NECKING AND LOCALIZATION IN PLANE STRESS / STRAIN

INTRODUCTION

The development of necking and localization in specimens subjected to a uniaxial tensile load are triggered by a bifurcation. This bifurcation occurs when a critical load is reached where the displacement path becomes unstable. Necking and its subsequent phenomena localization show the mechanics behind material and geometric non-linearities. These non-linearities which can make a specimen decrease in cross sectional area (necking), can induce strain localization at later stages. Specifically, necking occurs due to geometric non-linearities and localization occurs due to material non-linearities.

This report contains implicit finite element analysis of models with plane stress and plane strain elements, and of different materials. Two materials were used, an elasto-plastic and hyper-elastic material, to analyze their effect on necking and localization. The first part of this report contains some explanations about what bifurcation, necking, and localization is and the second part discusses the results of the analysis.

BIFURCATION

Bifurcation is defined as the loss of uniqueness of solution in a non linear problem. It corresponds to a sudden change in behavior when a critical load parameter (λ_c) is reached. In buckling or necking the bifurcation point is defined as the point when a compressive or tensile load reaches a maximum triggering a sudden change in displacement. Figure 1 shows the bifurcation paths for buckling (red) and necking (green). As the load increases from zero both paths are stable with displacements close to zero. The mathematical theoretical solution states that the load will increase with zero displacement until λc is reached (yellow solid line). In real life because of imperfections and in finite element because of approximations there will always be some displacement before the critical load is reached. This can be observed in the initial solid red and green lines. Once λ_c is attained, the paths will bifurcate into non unique solutions. The buckling path will become stable while that of necking will become unstable. Ahead the finite element results are presented which excellently capture this behavior.

Figure 1. Bifurcation Phenomena

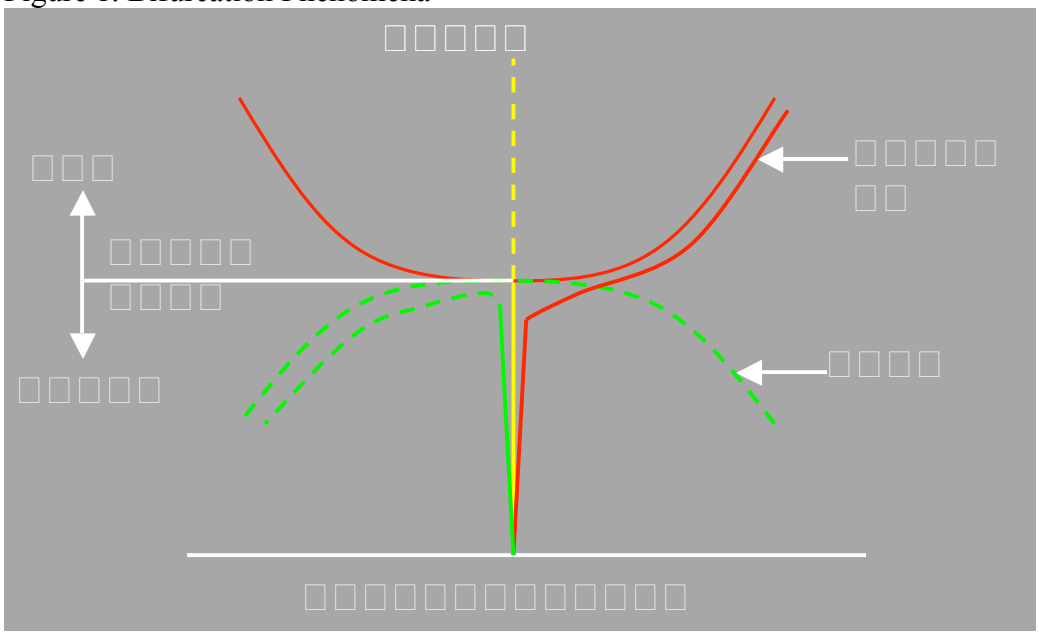

NECKING / LOCALIZATION

This reports aims to analyze two different bifurcation phenomena's. The first one is necking which depending on the material used might lead to the second bifurcation phenomena, strain localization.

- **Necking**:
  Necking occurs due to geometric non-linearities and can be observed as a decrease in cross-sectional area of a specimen under tensile load. If a specimen is loaded in tension as seen in Figure 2 it will undergo three stages that will culminate with necking. First, the behavior will be stable with a constant decrease in cross sectional area throughout the length of the specimen. When the critical load is reached bifurcation occurs and the center of the specimen will neck. In order to see this complete behavior the sides of the specimen must be under shear free boundary conditions (i.e. rollers on both edges). In lab experiments it is very hard to give shear free boundary conditions so fixed boundary conditions (clamped) are given at the edges which then force the specimen to start at the second step and go directly into necking behavior. The same is true for finite element analysis where boundary conditions play a crucial role. These boundary condition requirements will be discussed in more detail in the boundary condition section. The analysis performed in this report starts the model when the bifurcation that triggers necking occurs. Capturing the pre-necking behavior is much more involved and is not of much use since most real-life elements undergoing necking will be fixed at both ends (does not allow for pre-neck behavior).

Figure 2. Three stages of necking

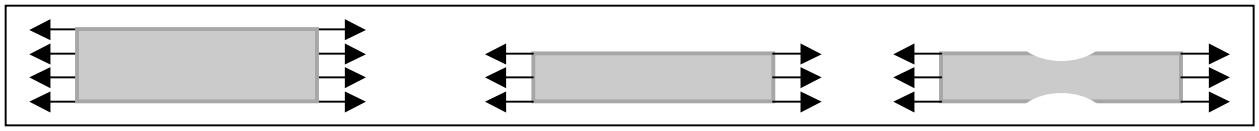

- **Localization:**
  Localization which occurs after necking is defined as a bifurcation phenomenon which creates diagonal shear bands in the necked area which eventually cause the specimen to fracture along these bands. These bands are formed because of plastic strain localization. Strain localization is due to the materials non-linear behavior. Not all materials that undergo necking will experience localization. A more detailed discussion on why certain materials undergo localization is presented in the next section. Figure 3 is an example of strain localization for a steel specimen.

Figure 3. Shear Bands Example

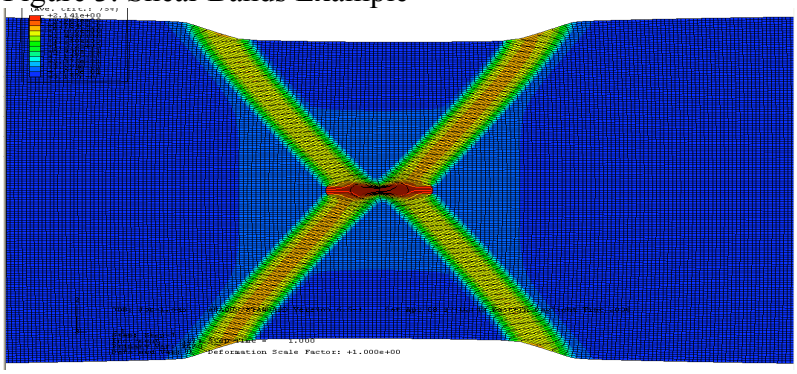

FE MODEL DESCRIPTION

- **Materials**
  - **Elastoplastic: Steel**
    An elastoplastic J_2 flow theory behavior was used to model the behavior of steel. An elastoplastic material experiences linear behavior until yield stress, where the material enters into the plastic range. The non-linear plastic behavior is defined by the following work hardening uniaxial equation:

$$\frac{\sigma}{\sigma_y} = \left(\frac{\sigma}{\sigma_y} + \frac{3G}{\sigma_y} \varepsilon \right)^n$$

$$G = \frac{E}{2(1+v)}$$

Where the stress σ is a function of strain ε. The following values were assumed for steel: yield stress "σ_y" of 50 ksi, modulus of elasticity "E" of 29,000 ksi, poisons ratio of 0.3, and hardening parameter "n" as 10.

Different "n" factors were analyzed but n=10 gave a smoother looking curve. The "G" is the elastic shear modulus which is a function of modulus of elasticity and poisons ratio. As mentioned before this material allowed the model to undergo necking and strain localization. Figure 4 shows the behavior of this elastoplastic:

Figure 4. Stress vs. Strain Curve

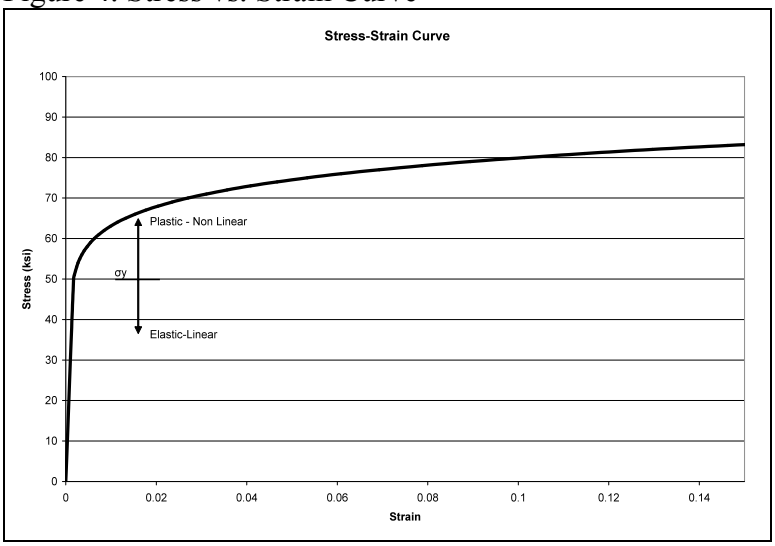

- **Hyper-Elastic (Arruda Boyce)**

The hyperelastic incompressible Arruda Boyce model was used as an example of a material that will cause necking in the specimen but will not allow for strain localization. The Arruda-Boyce model stress-strain relationship has the following form:

$$T_U = \frac{\partial U}{\partial \lambda_U} = 2(1-\lambda_U^{-3})\left(\lambda_U \frac{\partial U}{\partial \bar{I}_1} + \frac{\partial U}{\partial \bar{I}_2}\right),$$

$$U = \mu \sum_{i=1}^{5} \frac{C_i}{\lambda_m^{2i-2}}\left(\bar{I}_1^i - 3^i\right) + \frac{1}{D}\left(\frac{J_{e\ell}^2 - 1}{2} - \ln J_{e\ell}\right)$$

$$C_1 = \frac{1}{2}, \quad C_2 = \frac{1}{20}, \quad C_3 = \frac{11}{1050}, \quad C_4 = \frac{19}{7050}, \quad \text{and} \quad C_5 = \frac{519}{673750}.$$

$\lambda_1 = \lambda_U, \ \lambda_2 = \lambda_3 = \lambda_U^{-\frac{1}{2}}$ …for uniaxial tension

Where U is the strain energy potential, λ_U is the stretch in the uniaxial direction, and I_i are the deviatoric strain invariants. This model assumes full incompressibility ($J= \lambda_1 \lambda_2 \lambda_3=1$). The coefficient λ_m is referred to as the locking stretch. Approximately at this stretch the slope of the stress-strain curve will rise significantly. This model is also known as the eight-

chain model, since it was developed starting out from a representative volume element where eight springs emanate from the center of a cube to its corners. The values of the coefficients $C_1 \ldots C_5$ arise from a series expansion of the inverse Langevin function. The series expansion is truncated after the fifth term. The coefficient λ_m is referred to as the locking stretch. Approximately at this point the slope of the stress-strain curve will rise significantly. Figure 5 shows the stress-strain curve for the uniaxial form of the Arruda-Boyce model.

Figure 5. Uniaxial Tension – Arruda Boyce Model

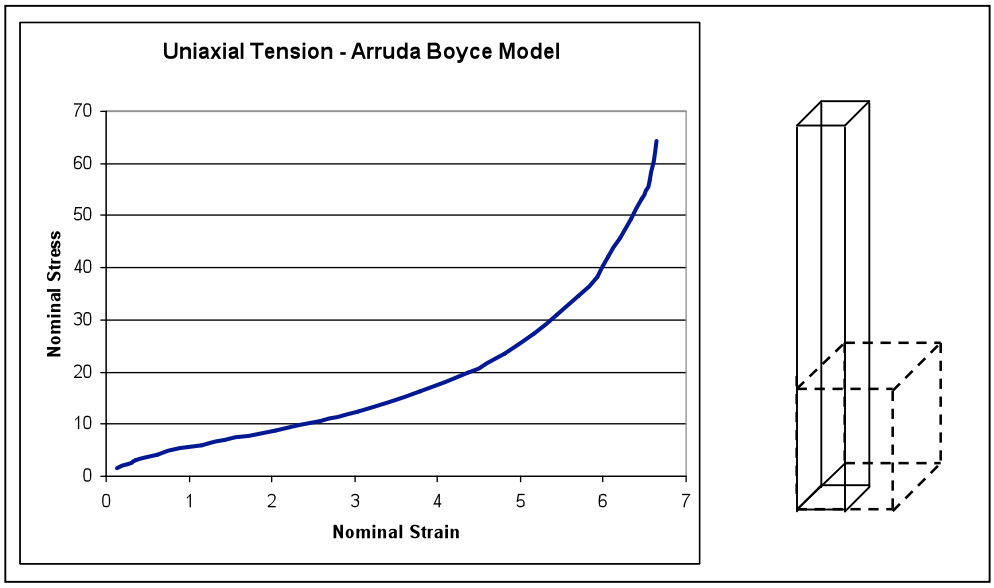

- **Elements & Meshing**
  Both plane stress and plane strain elements were used to analyze the model. They both provided similar results. The mesh had to be refined as much as possible in order to capture localization. A denser mesh was used in the middle section were localization occurs. Reduced integration was used to avoid volumetric locking.

- **Boundary Conditions**
  Defining the correct boundary conditions in the finite element model is crucial to capture the necking and localization phenomena's. As mentioned before to undergo through all the stages that lead to necking, shear free supports must be given at the edges of the specimen. Given that this is almost impossible, the analysis can be started right before necking occurs by either providing fixed boundary conditions or a geometric imperfection at the center of the model. If the geometric imperfection is used then rollers can be assigned to the edges providing a shear free edge support. Usually this geometric imperfection will be a small dip at each side of the plate on the center for a shell element analysis or a change in thickness at the center for a solid element analysis. This report was completed

using fixed boundary conditions, not geometric imperfections. The results should be very similar because they both have the same effect which is to trigger a concentration of stresses in the center of the specimen.

A trial run was performed to validate the results using neither a clamped support nor a geometric imperfection. The results were as expected where the plate experienced a constant decrease in thickness throughout the length without any necking or localization.

- **Non Linearities**
  This problem incurs both geometric and material non-linearities. The material non-linearities as discussed above arise from the non-linear behavior of stress as a function of strain. For the elasto-plastic material the analysis does not include material non-linearities until it reaches the yield stress were it changes to non-linear behavior. The hyper-elastic material is always non-linear. The geometric non-linearties arise from non-linear strains. The Abaqus step module has an option "Nlgeom" which allows the user to include the non-linear effects of large displacements.

RESULTS / DISCUSSION

- **Elasto-Plastic Model:**
  - **Plane Strain**
    For the stated conditions the plate was analyzed and the results are shown in Figure 6 (contours of plastic strain). Figure 6.a shows the preliminary plate before any displacements (dense mesh in middle section). Figure 6.b shows the initial strain formation at the upper and lower edges of the plate, and some other symmetrical accumulations of strains in the middle portion. Figure 6.c shows how the strain in the corners radiated inward and met with the ones previously found in the center. At this point the non-uniforms strains can be observed specially in the edge support (dark blue-smaller strain). Figure 6.d shows the circular formation of strains in the middle section right before localization occurs. This figure also shows how the whole plate is loaded (plastic strain) but the boundary edges have zero strains. This loading and unloading process is very important for localization. At Figure 6.e bifurcation occurs and there are early signs of shear band formations. This figure shows how the top and bottom edges of the center of the plate have lower plastic strains than the middle section from where the shear bands radiate diagonally. Figure 6.f is a close up of the shear bands already formed. Figure 6.g shows the whole specimen at the end of the analysis where in a real test it would have likely already fractured.

Figure 6. Elasto-Plastic: Plane Strain Case Evolution (PE contours)

a.

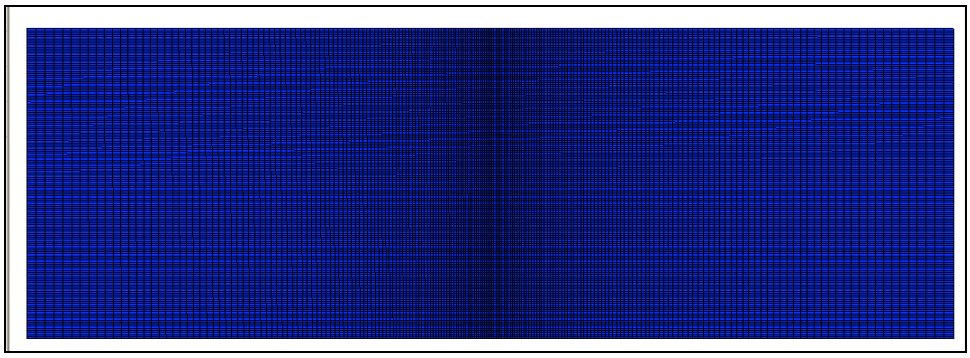

b.

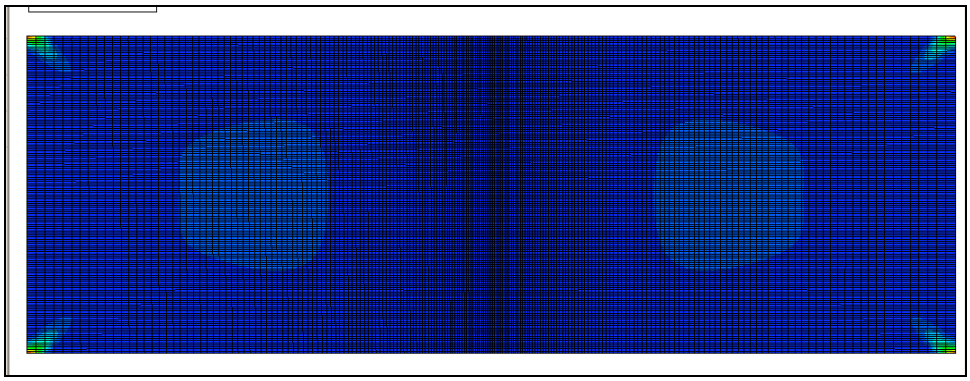

c.

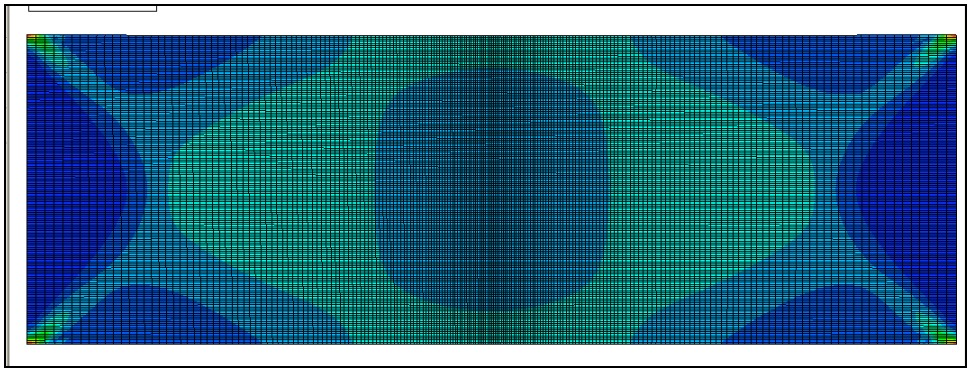

d.

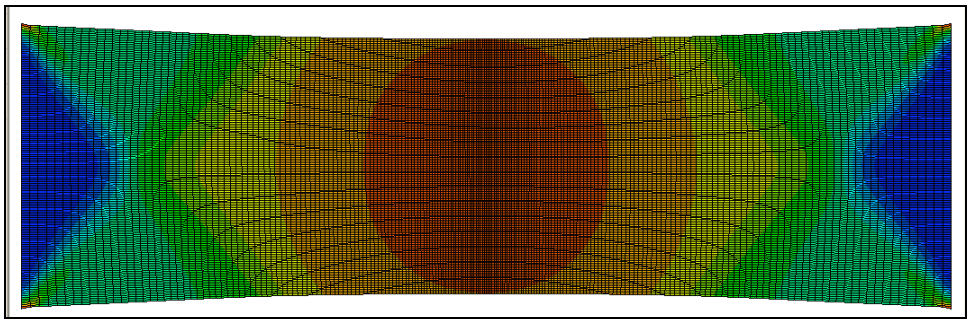

e.

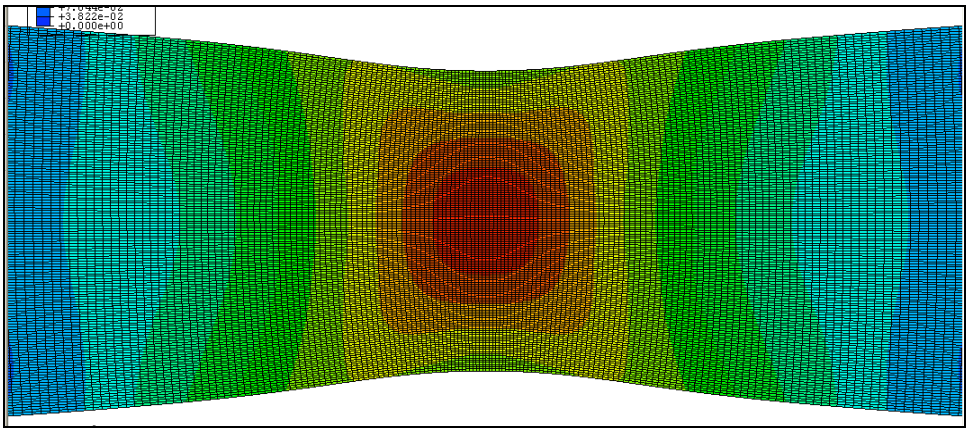

f.

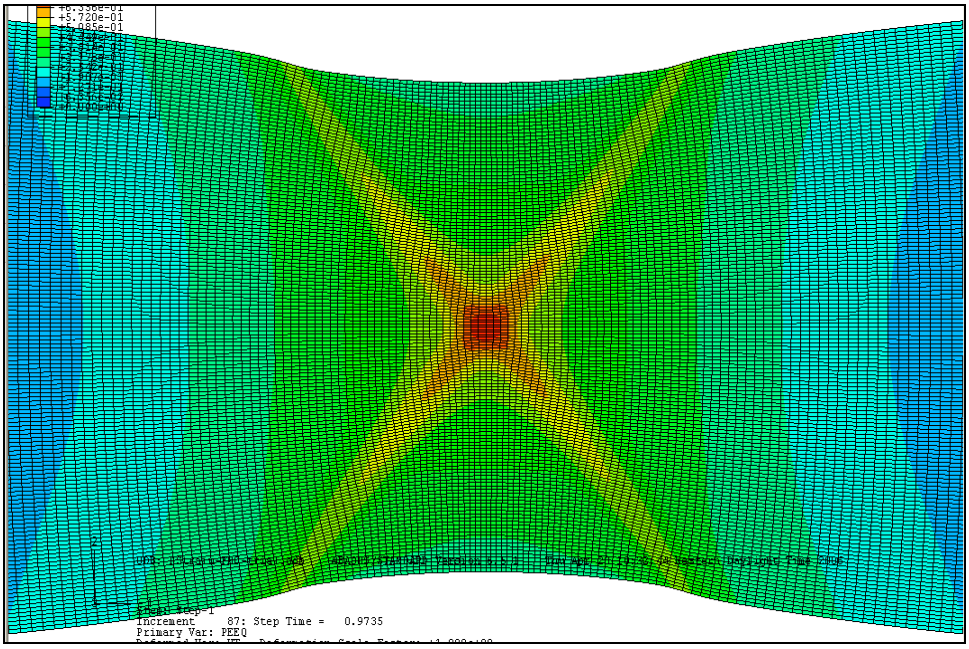

g.

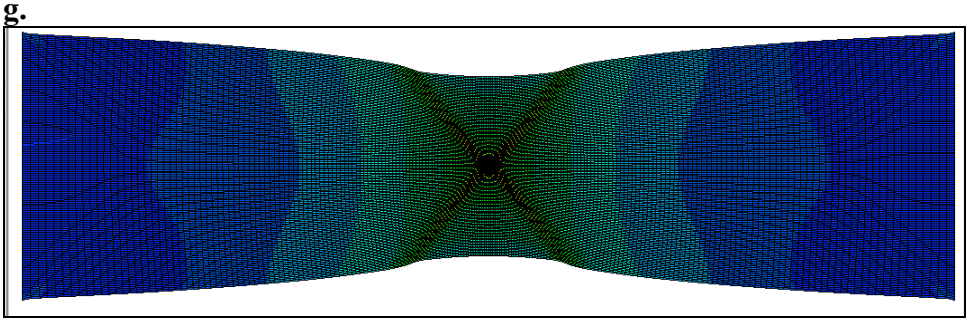

To better understand when the bifurcation occurs the following load curves were plotted. This curves shows the bifurcation that starts the strain localization. The following load curves are normalized both in the x and y axis by length and yield force, respectively. Figure 7 shows the normalized load curve for longitudinal displacement. The maximum load occurs at a

factor u/L of 0.083 with a normalized critical load of 1.7. Through previous research it has been shown that the actual bifurcation occurs just after the maximum load. This figure also shows the fundamental path which would be followed if localization would not have occurred. Figure 8 shows the normalized load curve for width displacement at a maximum u/w of 0.054.

Figure 7. Load Curve (u/L)

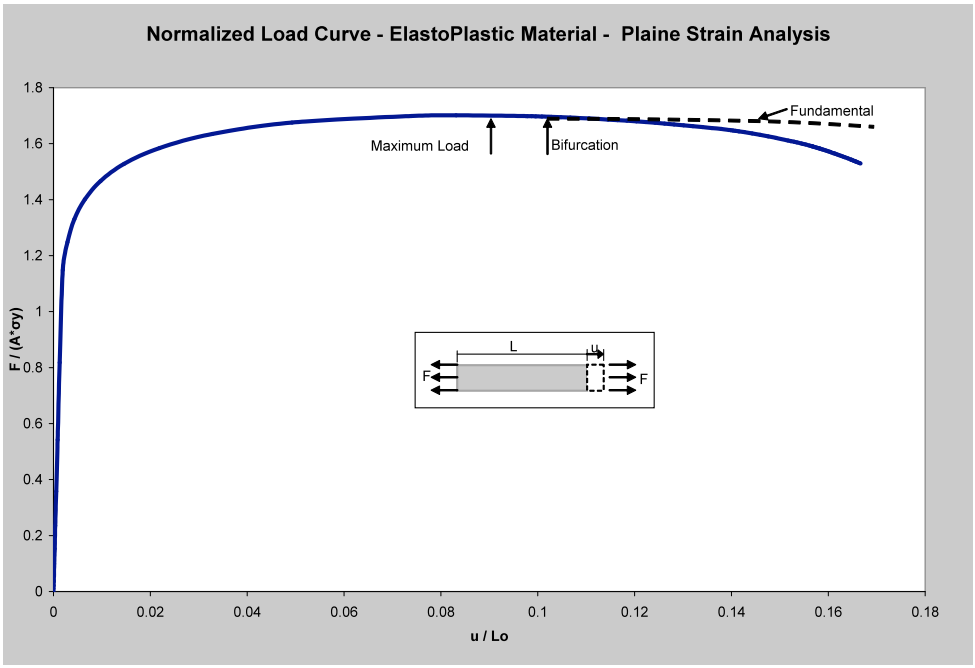

Figure 8. Load Curve (u/w)

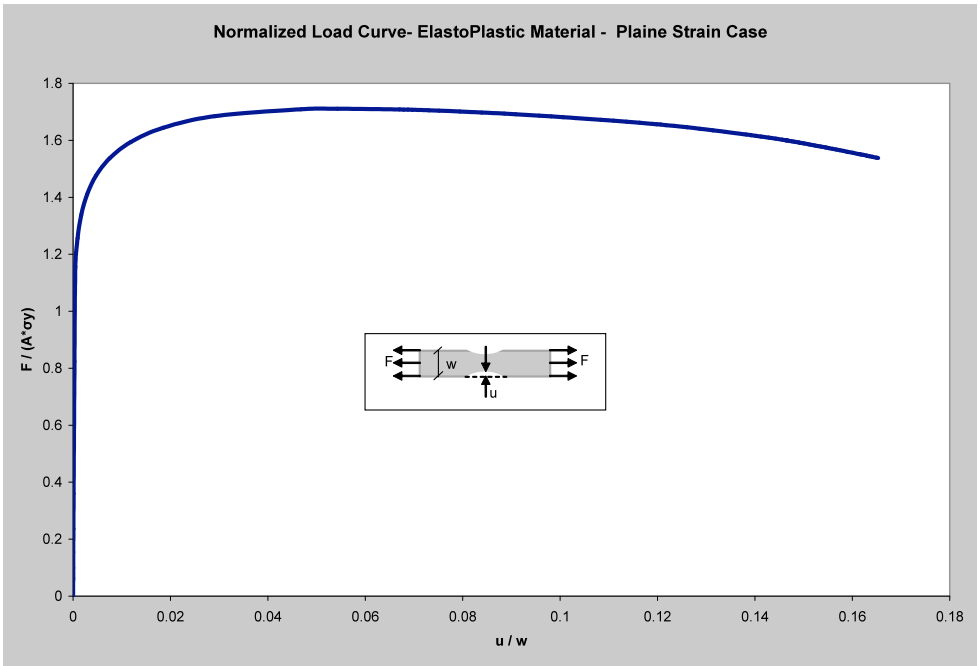

- **Plane Stress**

The plane stress case had similar results to the plane strain case. Figure 9 shows the plate with plane stress elements at the end of the analysis. The main difference between plane strain and plane stress is that in plane stress the shear bands are more pronunciated as can be seen by the slopes of the plate's edges at the end of the diagonals. This can also be observed by looking at the slope along any edge from the boundary to the point were localization occurs. In the plane strain case this slope is less gradual when compared to plane stress. Figure 10 shows the normalized curve with a maximum of u/L 0.089 very similar to plane strain. The maximum normalized critical load is of about 1.45. The curve after the bifurcation point which seems to be somewhat unstable does not provide any real physical meaning since a real specimen would be in the process of fracturing at this time for which a whole new analysis is needed.

Figure 9.Final Formation of Shear Bands (ElastoPlastic: Plane Stress)

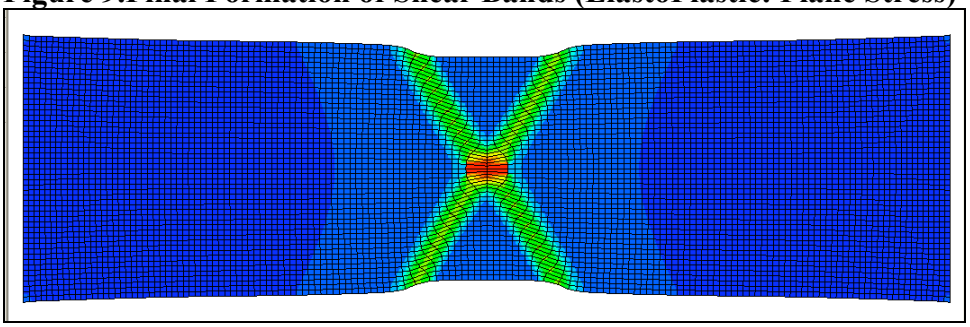

Figure 10. Normalized Load Curve

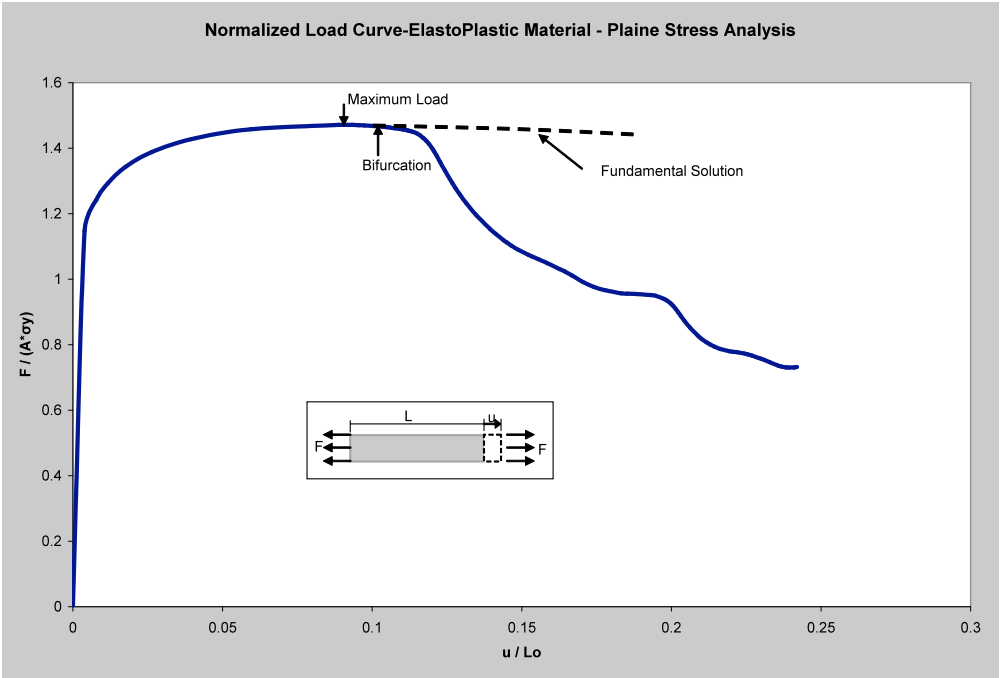

- **Hyper-Elastic Model:**

The hyper elastic (Arruda Boyce) material was used to explore necking without subsequent localization. Figure 11 shows the stages from beginning to end where no strain localizations can be observed. Figure 12 has the normalized curve for the width displacement which is not conclusive. This curve is linear up until u/w of 0.13 where it becomes an exponential curve. Given that Abaqus had to stopped the analysis after the elements width had become to small to continue integrations the second part of the curve could be due to errors of the finite element analysis. This behavior may also be due to the materials non-linearity. I was not able to find information of this type of analysis with a hyper-elastic material. Figure 13 shows the normalized curve for longitudinal displacements. This plot is linear with a change of slope. Again this change in slope which occurs at around u/L of 0.75 might signal an error. Nevertheless it can be concluded that for small displacements the Arruda-Boyce model shows an increasing linear behavior for necking.

Figure 11.Necking behavior of Hyper-elastic material (disp. contours)

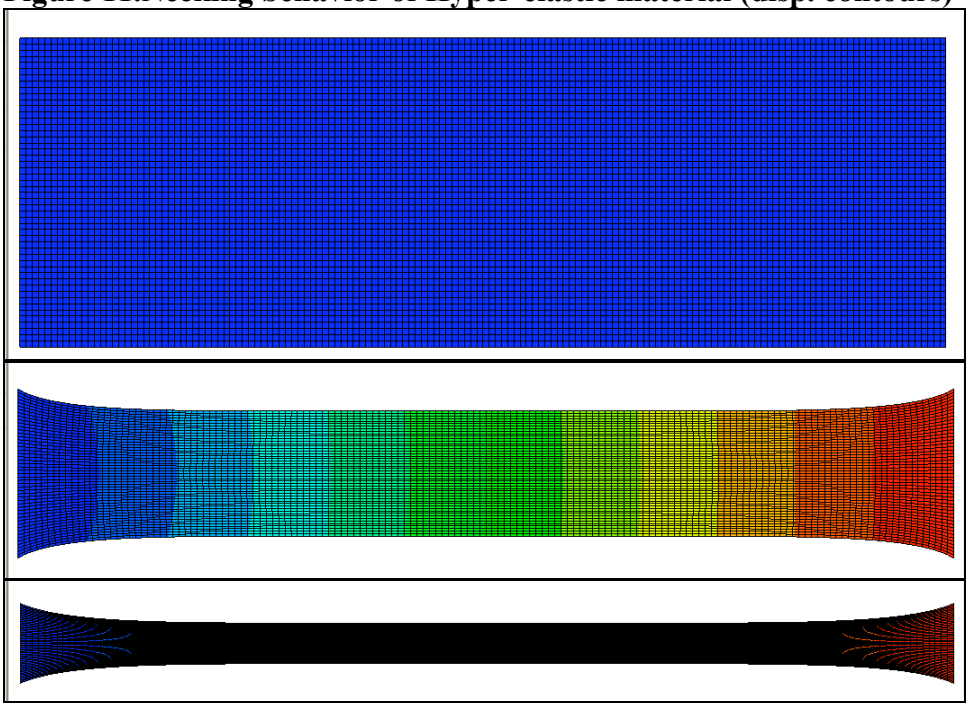

Figure 12. Normalized Load Curve-Arruda Boyce (u/w)

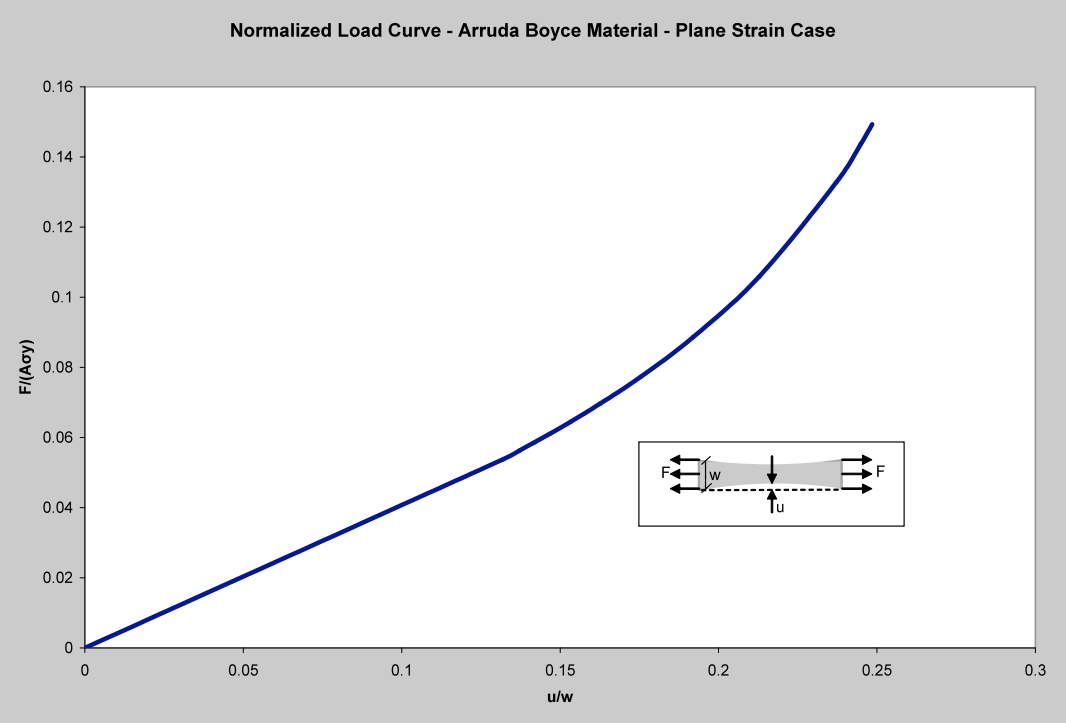

Figure 13. Normalized Load Curve-Arruda Boyce (u/L)

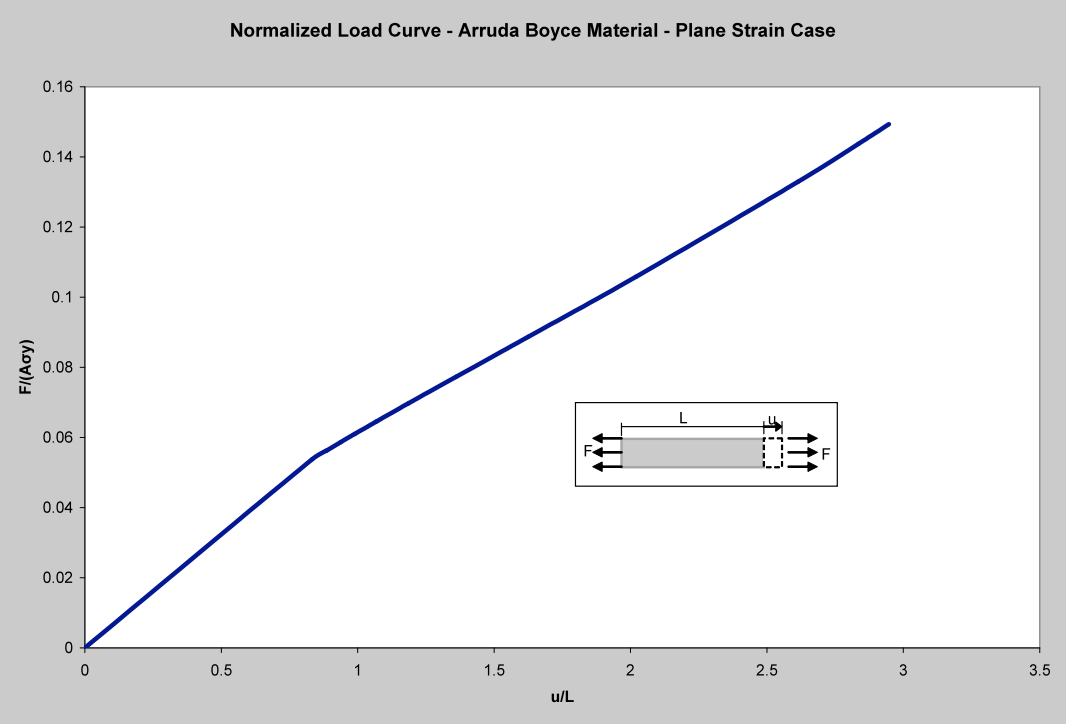

CONCLUSION

A complete analysis of necking and localization for plane strain and plane stress elements with different materials was presented in this report. The elasto-plastic (steel) material underwent necking and strain localization while the hyper-elastic (Arruda Boyce) only experienced necking as expected. The steel specimens reached a maximum load or critical load where bifurcation occurred and strain localization started. The critical load was reach at about a longitudinal displacement of 8.5% of the initial length, and it varied from 1.45 to 1.7 for plane stress and plane strain elements respectively. This strain localization culminated with the formation of shear bands. For the Arruda Boyce material only necking was observed due to the materials properties. The plane stress / strain tests had similar results. The analysis of 3-D models would have provided a better understanding of these phenomena but substantial computational power is needed to run this type analysis in a realistic time frame. Finally the results of this analysis where compared with past research in this field and there was a strong correlation for the elasto-plastic plane stress/strain results.

REFERENCES

1. **R. Hill, "Bifurcation Phenomena in the plane tension test", J. Mech. Phys. Solids, 1975, Vol. 23, pp. 239-264**

2. **R. Hill, "A general Theory of Uniqueness and Stability in elastic-plastic solids", J. Mech. Phys. Solids, 1958, Vol. 6, pp. 236-249**

3. **A. Needleman, "A numerical Study of Necking in Circular Cylindrical Bars", J. Mech. Phys. Solids, 1972, Vol. 20, pp. 111-127**

4. **V. Tvergaard, "Necking in Tensile Bars with Rectangular Cross-Section", Comp. Methods in App. Mech. And Eng., 103 (1993) 273-290**

5. **J.W. Hutchinson, "Post-Bifurcation Behavior in the Plastic Range", J. Mech. Phys. Solids, 1973 Vol. 21 pp. 163-190**

6. **S. Okazawa, T. Usami, H. Noguchim, F. Fujii, "Three Dimensional Necking Bifurcation in Tensile Steel Specimens", J. of Engineering Mechanics, April 2002, 479-486**

7. **V. Tvergaard, A. Needleman, "Flow Localization in the Plane Strain Tensile Test", J. Mech. Phys. Solids, 1981, Vol. 29, pp. 115-142**